Calculation of vibration–rotation spectra for rare gas–HCl complexes

David C. Clary and David J. Nesbitt

Citation: The Journal of Chemical Physics **90**, 7000 (1989); doi: 10.1063/1.456275
View online: http://dx.doi.org/10.1063/1.456275
View Table of Contents: http://scitation.aip.org/content/aip/journal/jcp/90/12?ver=pdfcov
Published by the AIP Publishing

Calculation of vibration–rotation spectra for rare gas–HCl complexes

David C. Clary[a)]
University Chemical Laboratory, Lensfield Road, Cambridge CB2 1EW, United Kingdom

David J. Nesbitt[b)]
Joint Institute for Laboratory Astrophysics, University of Colorado and National Bureau of Standards and Department of Chemistry and Biochemistry, Boulder, Colorado 80309-0440

(Received 27 September 1988; accepted 28 December 1988)

Calculations are described of spectra for the excitation of the bending and stretching vibrational–rotational energy levels in the van der Waals complexes of HCl with the rare gases Ne, Ar, Kr, and Xe. The calculations are performed using a basis set method, with distributed Gaussian functions being employed for the coordinate associated with the stretching of the rare gas atom. Intensities of combination and fundamental transitions for each of the low frequency modes are calculated for total angular momentum up to $J = 25$. Surprisingly large intensities are predicted for transitions to states with multiple vibrations excited in the bending mode. Promising comparisons are obtained with infrared spectra measured recently for the complexes of HCl with Ne and Ar at low temperatures.

I. INTRODUCTION

There has been significant progress in the development of experimental methods for measuring the spectra of small van der Waals molecules.[1,2] In particular, it has proved possible recently to measure the high-resolution far-infrared[3–8] and infrared[9–17] spectra involving the excitation of the vibration–rotation states of these complexes. These spectra promise to yield highly detailed information on the potential energy surfaces of these weakly bound systems.

The complexes of hydrogen halides with rare gases, especially Ar–HCl, have played a central role in the study of van der Waals molecules, both from the point of view of experiment[3–8,10,16–18] and theory.[19–24] Potential energy surfaces for these systems have been proposed by Hutson and Howard[21] by means of a multiproperty fitting of microwave spectra, far-infrared HCl pressure broadening coefficients, second virial coefficients and molecular beam scattering data. The fundamental vibrational bands of these complexes, together with their rotational constants and some other properties, have been calculated from these potentials by using close-coupling techniques.[21,24] Far infrared spectroscopic techniques[3–8] have been used to probe the fundamental vibrations for Ar–HCl and the agreement with the predictions from the Hutson and Howard M5 potential is good.

Furthermore, Howard and Pine[10] reported rotationally resolved infrared spectra for Ar–HCl in the H–Cl stretching region for a temperature of 127 K. Even more recently, the high-resolution infrared spectrum involving several vibrational–rotational bands has been measured for both Ar–HCl[17] and Ne–HCl[16] in a molecular beam corresponding to temperatures less than 10 K. These and other studies have elucidated the novel vibrational behavior of weakly bound complexes that arises from large amplitude motion on shallow potential surfaces. The spectroscopic manifestations of this behavior (e.g., large coriolis and Fermi resonance effects, internal rotations, etc.) are quite different from those which are observed in more stable, covalently bound molecules and new intuitions and theoretical methods of computation are needed.

An essential link between the potential energy surface and experiment for these van der Waals complexes is an efficient and general method capable of calculating accurately the vibrational–rotational bound states and the resulting spectra from a given potential energy surface. In particular, good calculations of line positions, intensities and widths are needed for the large numbers of total angular momenta J that are now being accessed in the experiments. The close-coupling approach[19,25,26] does provide very accurate energies for the fundamental vibrations. However, it is difficult and time consuming to calculate transition intensities with this technique and the method is not efficient enough to yield the full J-dependent spectra by using computers that are currently available. Furthermore, it is not straightforward to make the close-coupling approach completely automatic, which is an essential requirement when thousands of spectral lines need to be calculated.

The close-coupling method involves the numerical solution of the Schrödinger equation along the intermolecular coordinate. A more widely used approach is to use an expansion of the wave function in a coupled set of basis functions with the required eigenfunctions being obtained by matrix diagonalisation. This approach is quite straightforward for calculating the vibrational–rotational bound states of stable triatomic molecules.[27] Furthermore, very recently, basis set techniques have been used to calculate the spectra for some weakly bound systems including Ar–N_2,[28] N_2–N_2,[29] and rare gas–Cl_2.[30] Our own approach, described in Sec. II, does have several similarities to the methods used in these other computations but we are unaware of any previous attempt to predict the full J-dependent spectra for rare gas–HCl van der Waals complexes.

In this paper we describe a procedure that we have applied to the calculation of the full vibration–rotation spectra of atom–diatom van der Waals complexes. In particular, we report applications of the approach to the prediction of the far-infrared and infrared spectra for the complexes of HCl

[a)] 87–88 Visiting Fellow at the Joint Institute for Laboratory Astrophysics.
[b)] Staff Member, Quantum Physics Division, National Bureau of Standards.

 0021-9606/89/127000-14$02.10

with the rare gases Ne, Ar, Kr, and Xe. For Ar–HCl, we use a potential energy surface recently developed by Hutson[31] which was obtained through a fit to the far-infrared data of Robinson *et al.*[5–7] Potentials proposed by Hutson and Howard[21] are used for Ne, Kr, and Xe. In our calculations of the infrared spectra, which correspond to excitation of the rare gas(Rg)–HCl complex at frequencies close to that of HCl($v=1$), we make the assumption that the potential appropriate for Rg–HCl($v=0$) can be used in calculating the vibrational–rotational states. Recent comparisons of measured far-infrared[5–7] [i.e., Ar–HCl($v=0$)] and infrared[17] [i.e., Ar–HCl($v=1$)] spectra have demonstrated the accuracy of this approximation. The new feature of our computations is the prediction of the positions and intensities of the full J-dependent spectra for the Rg–HCl complexes. We hope that our predictions will facilitate the experimental search for observing new vibrational bands such as bending states excited with several quanta. This, in turn, may help elucidate the dynamics of internal rotation and rotational predissociation in these complexes. We also hope that our comparisons of computed and observed intensities will lead to a deeper understanding of the potential surfaces for these systems. The calculational method should be efficient and accurate enough to lead eventually to a highly accurate determination of the potential energy surfaces for systems such as these, a task we leave as a direction of future efforts.

In Sec. II we describe the approach for calculating spectra. The aim is to, first of all, obtain good sets of basis functions for the separate rare gas stretching and angular motions of the complex. Then a final "configuration–interaction" calculation is done in which the stretching and angular basis sets are coupled together. If the dipole moment or vibrational transition moment of the Rg–HCl complex is directed along the HCl bond, it is straightforward to calculate intensities for transitions between the different vibrational–rotational states. Section III describes the potential energy surfaces used. The recent high-resolution experiments demand a very high accuracy (<0.001 cm^{-1}) in the calculated energy levels and particular attention is paid to examining the accuracy of the method through numerical tests in Sec. IV. In this section, we also compare with previous close-coupling calculations of the fundamental vibrational energies. In Sec. V we present and discuss our predictions of spectra for the complexes of HCl with Ne, Ar, Kr, and Xe. We also pay particular attention to the comparison of our computed spectra with the infrared spectra recently measured for Ne–HCl and Ar–HCl using molecular beam techniques.[16,17] Conclusions are in Sec. VI, where the future possibilities of the approach are discussed.

II. COMPUTATIONAL TECHNIQUE

Details of the potential energy surfaces used to calculate the vibrational–rotational spectra of the Rg–HCl complexes are given in Sec. III. We here describe our approach for calculating the vibrational–rotational spectra of an atom–diatom complex from a given potential energy surface. The method is described for Rg–HCl complexes, although it is generally applicable to atom–diatom systems. We use a space fixed coordinate frame[32] as this makes the calculation of transition intensities particularly simple. In this frame, the HCl internuclear vector is **r** and the vector joining the Rg atom to the center of mass of the HCl molecule is **R**. We also have $\mathbf{R}\cdot\mathbf{r}=Rr\cos(\theta)$. The appropriate vibrational–rotational Hamiltonian is then

$$H=-\hbar^2/(2\mu R)\left[\frac{\partial^2}{\partial R^2}\right]R-\hbar^2/(2\mu' r)\left[\frac{\partial^2}{\partial r^2}\right]r + \mathbf{j}^2/(2\mu' r^2)+l^2/(2\mu R^2)+V(R,r,\theta)\,, \quad (1)$$

where μ and μ' are, respectively, the reduced masses of the Rg–HCl complex and the HCl molecule. Also, $\mathbf{j}^2$ and l^2 are, respectively, the rotational and orbital angular momentum operators associated with the rotation of **r** and **R** respectively. The potential energy surface is $V(R,r,\theta)$. The spherical polar angles describing the orientation of **r** and **R** in the space-fixed plane are (θ',ϕ') and (θ'',ϕ''), respectively.

Molecules such as hydrogen halides have vibrational frequencies two orders of magnitude larger than the HX rotational constants and nearly five orders of magnitude larger than the rotational constants of the Rg–HX complexes. Therefore, the effect of the vibrational (i.e., r) motion on the Rg stretching (i.e., R) and angular motion is small, and the HCl stretching motion will be effectively averaged over the low-frequency intramolecular vibrations and end-over-end rotational motions in the complex. Furthermore, the evidence from vibrational relaxation studies is that the translational–vibrational coupling terms in the potential are very small.[33] Added to this is that there have been reasonable determinations of the potential energy surface for the R and θ dependent part of the potential[21] but very little is known about the r dependent parts. We thus make the approximation that the bond distance for the HCl molecule can be held at its equilibrium value. This should be a very good approximation for determining the Rg–HCl($v=0$) vibrational–rotational energy levels. Furthermore, the evidence is that if should also work well for the Rg–HCl($v=1$) energy level spacings as the fundamental stretching and bending frequencies differed by less than 0.5 cm^{-1} in the far infrared[5–7] and infrared[17] studies on Ar–HCl. These considerations enable us to neglect the kinetic energy operator depending on $\partial^2/\partial r^2$ in Eq. (1) and we also set $(1/r^2)$ to a suitable expectation value and use the equilibrium value of r in $V(R,r,\theta)$. We emphasize, however, that if the r dependent part of the potential was determined to a reasonable accuracy then it would be straightforward to use an appropriate basis set to describe the r motion also. This has been done, e.g., by Tennyson and co-workers.[34]

We, therefore, wish to find the eigenvalues and eigenfunctions for the Hamiltonian

$$H=-\hbar^2/(2\mu R)\times\left[\frac{\partial^2}{\partial R^2}\right]R+B\mathbf{j}^2+l^2/(2\mu R^2)+V(R,\theta)\,. \quad (2)$$

We do this by first attempting to obtain a suitable basis set for the R and angular motion separately and then by coupling these basis functions together. First of all, the intermolecular potential is expanded as a Legendre series on a chosen grid in R

$$V(R,\theta) = \sum_{n=0}^{N} c_n(R) P_n(\cos\theta) \tag{3}$$

by integrating $V(R,\theta)$ using a Gauss–Legendre quadrature. The coefficients $\{c_0(R)\}$ are then taken as an effective stretching potential and a basis set of $n_{\rm str}$ distributed Gaussian functions[35] equally spaced on the grid $\{R_i\}$ are used to obtain the eigenfunctions

$$\Psi^k_{\rm str}(R) = \sum_{i=1}^{\rm nstr} d_{ki} (2\alpha/\pi)^{1/4} \exp[-\alpha(R-R_i)^2]/R \tag{4}$$

of the "stretching" Hamiltonian

$$H = -\hbar^2/(2\mu R)\left[\frac{\partial^2}{\partial R^2}\right] R + c_0(R)\,. \tag{5}$$

The exponent α is varied to give the lowest eigenvalue with minimum energy and the $\{R_i\}$ were placed between the boundary points R_1 and R_2. The matrix elements with this basis set are computed using Gauss–Hermite quadrature. The $N_{\rm str}$ contracted eigenfunctions $\{\Psi^k_{\rm str}(R), k=1,N_{\rm str}\}$ with lowest energy are stored for later use in the full direct product stretching–angular basis set. The same set of contracted stretching eigenfunctions are used for all values of J.

With the stretching basis set obtained in the above way, the next step is to find an optimum angular basis set for each value of the total angular momentum J. This is done with respect to the stretching function $\Psi^{k=1}_{\rm str}(R)$ with lowest energy. Thus, the Hamiltonian

$$H = B\mathbf{j}^2 + \left\langle \Psi^1_{\rm str}(R)\,|\,l^2/(2\mu R^2) + \sum_{n=1}^{N} c_n(R) P_n(\cos\theta)\,|\,\Psi^1_{\rm str}(R)\right\rangle \tag{6}$$

is diagonalized with the angular basis

$$y^{JMp}_{lj}(\theta',\phi',\theta'',\phi'') = \sum_{m_j}\sum_{m_l} C(j,l,J,m_j,m_l,M) \times Y^{m_j}_j(\theta',\phi') Y^{m_l}_l(\theta'',\phi'')\,, \tag{7}$$

where $C(j,l,J,m_j,m_l,M)$ is a Clebsch–Gordan coefficient.[36] Here, M is the projection of $\mathbf{J}$ along the space-fixed z axis and is arbitrarily set to zero in the energy level calculations. The size of the basis set is determined by the maximum value of j, $j_{\rm max}$, and, consequently, the largest possible value of l is $J+j_{\rm max}$ for a given J. The Hamiltonian matrix with this basis set divides into two uncoupled blocks which depend on whether the parity $p = (-1)^{j+l}$ is positive or negative. The $N_{\rm ang}$ angular eigenfunctions of the form

$$\Psi^{kJMp}_{\rm ang}(\theta',\phi',\theta'',\phi'') = \sum_j \sum_l d^k_{lj}\, y^{JMp}_{lj}(\theta',\phi',\theta'',\phi'') \tag{8}$$

with lowest energy are kept to use in the final wave function expansion.

With the near-optimum basis functions calculated in the way described above, the final wave function is expanded in the coupled stretching–angular form

$$\Psi^{nJMp}_f(R,\theta',\phi',\theta'',\phi'') = \sum_k \sum_{k'} d^{nJMp}_{kk'} \Psi^{k'JMp}_{\rm ang} \times (\theta',\phi',\theta'',\phi'') \Psi^k_{\rm str}(R) \tag{9}$$

and the full Hamiltonian of Eq. (2) is diagonalized. The basis set is kept to a reasonable size by imposing the restrictions $k \leqslant N_{\rm str}$, $k' \leqslant N_{\rm ang}$ and $k + k' \leqslant N_x$ for $k,\ k' > 1$. Here, N_x is introduced to reduce the number of "cross terms" in the basis set of Eq. (9). The evaluation of the matrix elements with this basis set is simple as all the required integrals have been computed in the previous separated calculations for the angular and stretching motion. This simplification is possible because of the separable expansion of the potential of Eq. (3).

Since the infrared chromophore is HCl, the infrared transition moment of the complex is assumed to lie instantaneously along the HCl bond. The evaluation of the transition matrix elements is then particularly easy as we are using a contracted space-fixed basis set for the angular functions. The transition amplitude is proportional to

$$A(n,J,p,M\rightarrow n',J',p') = |\langle \Psi^{nJMp}_f(R,\theta',\phi',\theta'',\phi'')\,| \times Y^0_1(\theta',\phi')\,|\,\Psi^{n'J'Mp'}_f \times (R,\theta',\phi',\theta'',\phi'')\rangle|^2\,. \tag{10}$$

Evaluation of the matrix element

$$\langle y^{JMp}_{lj}(\theta',\phi',\theta'',\phi'')\,|\,Y^0_1(\theta',\phi')\,|\,y^{J'M'p'}_{l'j'}(\theta',\phi',\theta'',\phi'')\rangle = \delta(l,l')\sum_{m_j}\delta(m_l,M-m_j) C(j,l,J,m_j,m_l,M) \times C(j',l',J',m_j,m_l,M) \times \{[(2j'+1)3]/[(2j+1)]\}^{1/2} \times C(j',1,j,m_j,0,m_j) C(j',1,j,0,0,0) \tag{11}$$

together with appropriate matrix transformations gives the transition amplitudes. The form of the Clebsch–Gordan coefficients in Eq. (11) imposes the following selection rules:

$$J \rightarrow J' = J \pm 1$$

and

$$J \rightarrow J' = J$$

with the parity change $p \rightarrow p' \neq p$.
The M-summed transition amplitude

$$A(n,J,p\rightarrow n',J',p') = \sum_M A(n,J,p,M\rightarrow n',J',p') \tag{12}$$

is then given a Boltzmann weighting according to the energy and degeneracy of the initial state (n,J,p) and the temperature considered.

The approximation of placing the dipole or vibrational transition dipole along the HCl bond is expected to be good on the basis of previous *ab initio* and multipole moment treatments of rare gas hydrogen halide molecules (see, e.g., Ref. 37). The approximation will become less accurate along the series Ne, Ar, Kr, Xe as the polarizability increases. However, the induced moments only make a contribution of less than 10% even for the Ar–HCl dipole moment.[6] For infrared experiments that excite the HCl stretch in the complex it is the dipole derivative with respect to the HCl coordinate r that gives the transition. Here, the same considerations apply, although it is possible that the induced moments will now be more important as the quadrupole moments of hydrogen halides are more sensitive to r than the

dipole moment.[38] It is probable that high-quality *ab initio* calculations are required to make more definitive statements on these matters.

The above procedures were incorporated into a general and automatic computer program for calculating the far infrared and infrared spectra of atom–asymmetric diatom systems. All that is required to run the program is a suitable potential energy surface, atomic masses, rotational constant of the monomer and certain simple control parameters described above. Almost all the computer time goes in to the diagonalization of the configuration interaction matrix corresponding to the wave function expansion of Eq. (9). A typical running time to produce the complete spectrum for Ne–HCl up to $J = 20$ (appropriate for a temperature of 10 K) was 3 h on a VAX 8600; in this calculation the size of the largest matrix to be diagonalized was 330.

III. POTENTIAL ENERGY SURFACES

For Ne–HCl we used the potential energy surface M4 of Hutson and Howard.[21] We used the M5 potentials for Kr and Xe obtained by the same authors.[21] For Ar–HCl we used a "M6C" potential recently derived by Hutson[31] as a fit to the far infrared spectroscopic constants of Robinson *et al.*[5–7] This potential gives almost perfect agreement with the fundamental vibrational frequencies, B rotor constants, coriolis splittings and expectation values of the vibration–rotation wavefunction over $P_1(\cos\theta)$ and $P_2(\cos\theta)$ observed experimentally[5–7] for Ar–HCl. The M6C potential is of the Maitland–Smith form

$$V(R,\theta) = \epsilon(\theta)(6x^{-n} - nx^{-6})/(n-6)\,, \qquad (13)$$

where

$$x = R/R_m(\theta)\,,$$

$$n = m(\theta) + \gamma(x-1)$$

and the parameters $\epsilon(\theta)$, $R_m(\theta)$ and $m(\theta)$ are all expanded in a Legendre series. The appropriate parameters are given in Table I. The potentials for all four systems have an absolute minimum for the linear Rg–HCl geometry, but also have a secondary minimum for the linear Rg–ClH geometry. Both the well depth and the anisotropy in the potentials increase[21] along the series Ne, Ar, Kr, Xe. All the calculations reported here refer to ^{35}Cl.

TABLE I. Parameters for the M6C potential [see Eq. (13)].

Parameter	Value
ϵ_0[a]/cm^{-1}	125.591
ϵ_1/cm^{-1}	14.277
ϵ_2/cm^{-1}	35.879
ϵ_3/cm^{-1}	− 1.278
m	14.88
γ	9
R_{m0}/Å	3.8627
R_{m1}/Å	0.0742
R_{m2}/Å	− 0.0866
R_{m3}/Å	0.1945

[a] The $\epsilon(\theta)$ function and the $R_m(\theta)$ function of Eq. (13) are expanded in the form $\epsilon(\theta) = \Sigma_{k=0}^{3}\,\epsilon_k P_k\cos(\theta)$ and $R_m(\theta) = \Sigma_{k=0}^{3}\,R_{mk}P_k\cos(\theta)$.

The van der Waals vibrations of the Rg–HCl complexes can be divided into three different types. The "Σ stretching vibration" refers to excitation in the rare gas-stretching coordinate R. The "Σ bending vibration," which refers to a hindered rotation of the HCl with no projection of angular momentum on the intermolecular axis, correlates with the $(j = 1, K = 0)$ eigenfunction of the HCl monomer in the limit of no anisotropy in the Rg–HCl potential energy surface. Here K is the projection of both **J** and **j** along the body-fixed vector **R**. In the limit of a very deep well in the potential with a large relative anisotropy, this state correlates with the linear triatomic vibrational state (02^00). In practice, the vibration lies somewhere between these two extremes; J and p are the only good quantum numbers for these systems. The "Π bending vibration" refers to a rotation of the HCl perpendicular to the intermolecular axis and correlates with $(j = 1, K = \pm 1)$ and (01^10), respectively. This state must have $J \geqslant 1$ and can have positive or negative parity p. Thus, there are two states with the same J but slightly different energies and these are denoted by Π^+ and Π^-. Note that + and − here refer to the *spectroscopic* parity $(-1)^J p$. Transitions with $\Delta J = \pm 1$ are possible between all the Σ and Π^+ states giving the normal P and R branch transitions. However, transitions with $\Delta J = 0$ are possible for the $\Sigma \rightarrow \Pi^-$ and $\Pi^+ \rightarrow \Pi^-$ transitions, and these produce Q branches.

IV. NUMERICAL TESTS

Our aim in the calculations is to predict the full J dependent spectra for the Rg–HCl complexes as accurately as possible with the best potential energy surfaces and computer facilities available to us. Since our main interest is in making detailed comparisons with infrared spectra obtained in supersonic jets, most of the spectra we report are for a temperature of 10 K. These temperatures are low, but still warm enough to populate a fairly large number of J levels significantly. It is, therefore, important to use a balanced basis set that gives a good convergence for each value of J. It is quite easy to get highly converged energy levels for $J = 0$, but the size of the basis does rise considerably with J, and thus considerable care is needed in examining the convergence of the energy levels. In contrast, the transition intensities, which are the main interest here, are not so sensitive to the quality of the basis sets.

The previous published close-coupling calculations[21] of Hutson are for $J = 0$ and 1 only, and are expected to be accurate to 0.001 cm^{-1}. In Table II we compare some of our

TABLE II. Comparison of frequencies (in cm^{-1}) calculated using the basis set and close-coupling (CC) (Refs. 21 and 31) methods for the complexes of HCl with Ne, Ar, Kr, and Xe.

	Ne		Ar		Kr		Xe	
Mode	Basis	CC	Basis	CC	Basis	CC	Basis	CC
Σ bend	16.681	16.681	23.659	23.658	29.667	29.663	46.689	46.686
Σ stretch	20.026	20.026	32.435	32.433	33.290	33.290	33.790	33.785
Π^- bend ($J = 1$)	23.733	23.733	34.039	34.039	41.240	41.241	51.498	51.498

calculations for the fundamental frequencies associated with the Σ bend, Σ stretch, and Π^- bending vibrations with those obtained in the close-coupling calculations.[21,31] The basis set used in these particular calculations had the parameters $N_{str} = 26, j_{max} = 8, N_x = 31, N_{ang} = 15$. This gives a total basis set size of 330 for the $J = 1$ calculations with even parity. It can be seen that our basis set calculations give frequencies that agree to all six figures with the close-coupling results for Ne–HCl, and this is an excellent test of the computer codes. The agreement is still very good for Ar–HCl, with only our calculations for the Σ stretch having a frequency of 0.002 cm^{-1} above the close-coupling result. For all four systems, the agreement for the Π^- state is excellent. The accuracy of our calculations for the Σ bend and Σ stretch levels does appear to degrade along the series Ne, Ar, Kr, Xe as the anisotropy and well depths become larger. For example, for Xe–HCl, the Σ stretch has a frequency 0.005 cm^{-1} above the close-coupling result. However, the overall agreement between the basis set and close-coupling results is still very promising and does suggest that the basis set methods will be very useful for accurate spectroscopic studies on these types of molecules. In particular, they have the advantage that the full J-dependent spectra can be predicted quite easily for experimentally realistic conditions.

To examine the convergence of the energy levels in more detail for higher values of J, we present in Table III our energies for the first 13 levels of Ar–HCl that we calculated with three different basis sets for $J = 5$. Although we have assigned quantum numbers and types of vibration to these levels, we should emphasize that these labels are only very approximate in some cases due to the extreme mixing between several basis functions. It can be seen from these tables that most of the levels have energies which are stable with respect to increasing the basis set. However, there are some combination and overtone bands which are not so well converged. These include the Σ bend + Σ stretch combination band and the doubly excited Π and Δ states ($j = 2, K = +1$) and ($j = 2, K = \pm 2$) overtones. However, providing that the basis set is balanced with respect to all J values, then quite reasonable spectra can still be obtained for these levels in the sense that the error in the energy levels is the same for each J value. This point is illustrated in Table IV where the convergence with respect to basis set is compared for $J = 5$ and $J = 6$ for certain levels which proved difficult to converge. It can be seen that the relative errors are almost the same in every case for both $J = 5$ and $J = 6$. Thus, although the absolute values of each of the spectral lines might be in error by as much as 0.02 cm^{-1} for one or two bands, the spacings between the lines in that band, and the appearance of the spectra, is predicted much more accurately. We emphasize that it is only for certain of the higher lying levels that convergence of the energies proves a problem and the transition intensities involving all levels are not sensitive to changes in the basis set.

TABLE III. Convergence of energy levels (in cm^{-1}) with respect to basis set size for Ar–HCl with $J = 5$. For definition of the parameters N_{str}, N_{ang}, and N_x see the discussion following Eqs. (5), (7), and (9), respectively.

Level	A[a]	B[b]	C[c]
Fundamental	− 114.7062	− 114.7064	− 114.7065
Σ bend	− 90.9150	− 90.9235	− 90.9295
Σ stretch	− 82.3772	− 82.3775	− 82.3775
Π^+ bend	− 80.7058	− 80.7072	− 80.7072
Σ bend + Σ stretch	− 65.6165	− 65.6584	− 65.6889
Σ stretch ($n = 2$)	− 56.9678	− 56.9686	− 56.9690
Σ stretch + Π^+ bend	− 51.2213	− 51.2244	− 51.2249
($j = 2, K = 0$)	− 46.4441	− 46.4467	− 46.4488
($j = 2, K = 1$)	− 44.7966	− 44.8252	− 44.8463
($j = 2, K = 2$)	− 38.5848	− 38.6467	− 38.6939
Σ stretch ($n = 3$)	− 34.9316	− 34.9352	− 34.9376
($j = 3, K = 0$)	− 34.8246	− 34.8253	− 34.8254
Σ stretch ($n = 2$) + Σ bend	− 27.5990	− 27.6046	− 27.6062

[a] $N_{str} = 24, N_{ang} = 13, N_x = 29$.
[b] $N_{str} = 25, N_{ang} = 14, N_x = 30$.
[c] $N_{str} = 26, N_{ang} = 15, N_x = 31$.

V. CALCULATIONS OF SPECTRA

The main new feature of this work is to examine the intensities of the lines in the spectra corresponding to the excitation of the low-lying stretching and bending vibrations in the Rg–HCl complexes. For each molecule there are several thousand possible lines, even at a temperature of 10 K, and the clearest way of presenting the data is through graphical representation. Therefore, most of this section will concentrate on the presentation and discussion of spectra rather than comparison between tabulated numbers. We consider the Ne, Ar, Kr, and Xe–HCl complexes individually as their spectra have several different features. We also compare our results in some detail with the infrared spectra obtained by Lovejoy and Nesbitt for a temperature close to 10 K for Ne–HCl[16] and Ar–HCl.[17] The far-infrared data on Ar–HCl that has been published[4–8] has not included intensity information so we do not make detailed comparison with that work. There has also been an infrared spectrum measured by Howard and Pine[10] for Ar–HCl at 127 K. We did not perform calculations with enough J states to do a proper comparison with the data for this temperature.

As the potentials used in our calculation did not have a dependence on the vibrational HCl coordinate r, we do not calculate the absolute frequency of absorption for infrared spectroscopy, which will be close to, although not exactly the same as, the HCl($v = 0 \rightarrow 1$) absorption frequency. To

TABLE IV. Comparison of energy level convergence as a function of basis set for Ar–HCl with $J = 5$ and 6.[a]

	$[A-C]/cm^{-1}$		$[B-C]/cm^{-1}$	
Level	$J = 5$	$J = 6$	$J = 5$	$J = 6$
Σ bend	0.0145	0.0151	0.0060	0.0060
Σ bend + Σ stretch	0.0724	0.0742	0.0305	0.0311
Doubly excited Π bend ($j = 2, K = 1$)	0.0497	0.0515	0.0211	0.0217
Doubly excited Δ bend ($j = 2, K = 2$)	0.1091	0.1083	0.0472	0.0472

[a] Calculations A, B, and C have the basis set parameters ($N_{str} = 24$, $N_{ang} = 13$, $N_x = 29$), ($N_{str} = 25$, $N_{ang} = 14$, $N_x = 30$) and ($N_{str} = 26$, $N_{ang} = 15$, $N_x = 31$), respectively.

translate our reported spectra to infrared spectra it is necessary to add the experimental fundamental frequency for Rg–HCl ($v = 0 \rightarrow 1$) to our calculated frequencies. To translate the spectra to the far infrared it is simply necessary to consider all frequencies above 0 cm^{-1}, neglecting those with negative frequency.

A. Ne–HCl

Figure 1 presents our calculated spectrum for Ne–HCl at a temperature of 10 K. At this temperature, the intermolecular vibrations are fully cooled and hence the Ne–HCl molecule is originally in its ground vibrational state. In the experiments there is typically a natural abundance mixture of 90% of ^{20}Ne and 10% of ^{22}Ne. We have carried out computations with both these isotopes and the lines in the spectrum have been weighted accordingly. The spectra also do not include any lines above the dissociation limit into Ne + HCl as these will be broadened by rotational predissociation and the intensities will be much reduced. From the point of view of spectra at 10 K, these lines are of minor importance, but their significance will increase for spectra at higher temperatures. The Ne–HCl spectra show four main bands. The one at 0 cm^{-1} shows the expected regularly spaced P and R lines of the fundamental band. The bands centered on 16.681, 20.026, and 23.733 cm^{-1} are the Σ bend, Σ stretch, and Π bend, respectively. It is worth noting that the infrared spectra of Lovejoy and Nesbitt[16] gives these bands centered on 15.6845, 20.8549, and 22.5245 cm^{-1} respectively, in quite good agreement from the predictions with the Hutson–Howard M4 potential. Each of the Π^+ bend, Σ bend, and the Σ stretch exhibit Fermi resonance or coriolis mixing which lead to perturbed P and R branch structures. The Π bend also has a sharp Q branch associated with the $\Delta J = 0$ transitions from the ground state into the corresponding Π^- levels. There is no nearby vibration of the correct symmetry to interact with the Π^- levels, and hence the Q branches should essentially be unperturbed.

The experimental infrared intensity ratio for the fundamental (HCl stretch), Σ bend, Σ stretch, and Π bend has been estimated as[16] 1.0:7.6:3.1:7.6 by averaging the $R(5)$ and $P(5)$ lines. Our calculations give this ratio as 1:6.5:2.6:7.2, which is a very good agreement considering the sensitivity of the intensities to the potential energy surface and the difficulties in extracting accurate intensities from experimental data. There are two points of particular interest to emphasize about these intensities for Ne–HCl. For the fundamental band to have any intensity at all, the anisotropy of the Ne–HCl potential must mix the $j = 0$ and $j \geqslant 1$ HCl basis functions in the vibration–rotation wave function for the level with lowest energy. Otherwise, if there is no anisotropy, the strict $j = 0 \rightarrow 1$ selection rule will insure a zero intensity for this transition. The fact that the fundamental band is calculated and observed to have a much lower intensity than the other bands reflects the relatively weak anisotropy in the potential energy surface for Ne–HCl. However, the anisotropy in the potential is not weak enough such that the fundamental band in Ne–HCl cannot be observed. The other striking feature about the intensities is that the intensity of excitation of the Σ stretching band is quite strong. This is due to the fact that the Σ stretch is very close in energy to the HCl($j = 1$) energy, and thus can "borrow" oscillator strength from the Σ and Π^+ levels from strong Fermi and coriolis interactions respectively.

Figures 2–4 show enlarged sections of the calculated spectra for excitation of the Σ bend, Σ stretch, and Π bend modes. The Σ bending mode (Fig. 2) has a band head in the R branch at the transition $J = 11 \rightarrow 12$. This reflects the fact that the B rotor constant for this mode, 0.0880 cm^{-1} is smaller than that for the ground state, 0.090 85 cm^{-1}. This is partly due to the fact that the Σ stretching mode has a frequency quite close to that for the Σ bending mode and, consequently, the Σ bend has some excited Ne stretch character which gives a smaller rotor constant. As is shown in Fig. 3 the Σ stretching mode itself has a band head in the R branch at the transition $J = 5 \rightarrow 6$, which is at a smaller value of J

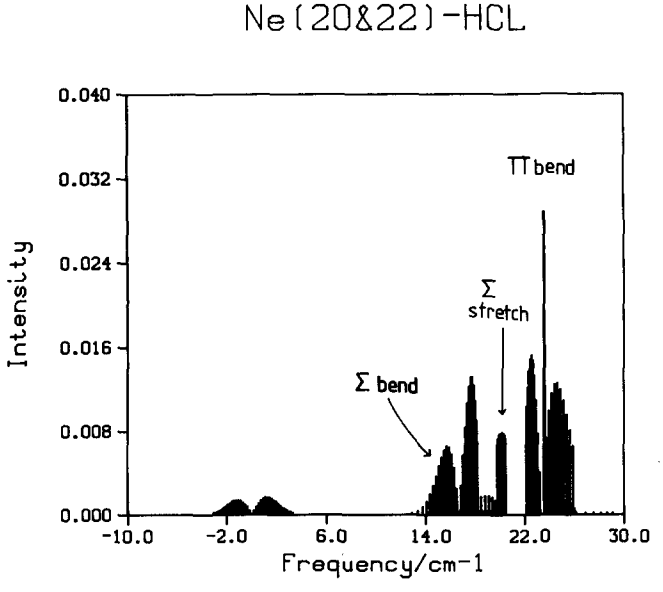

FIG. 1. Spectrum for Ne–HCl at 10 K.

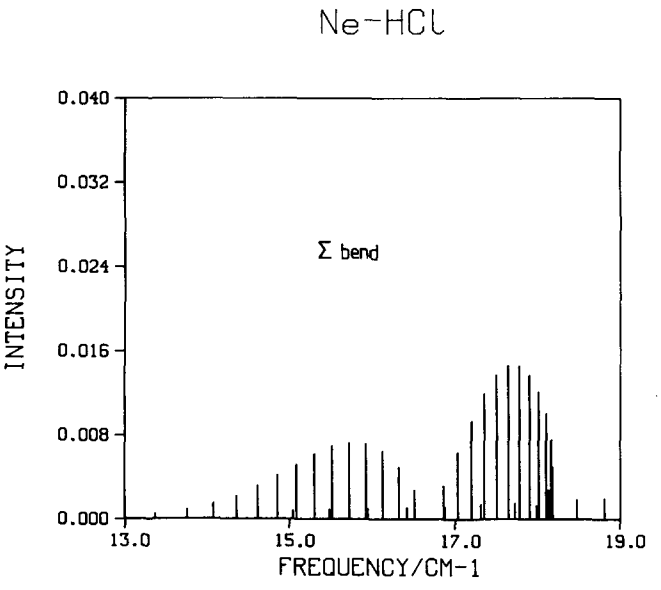

FIG. 2. Σ bend of Ne–HCl (P and R branch) at 10 K.

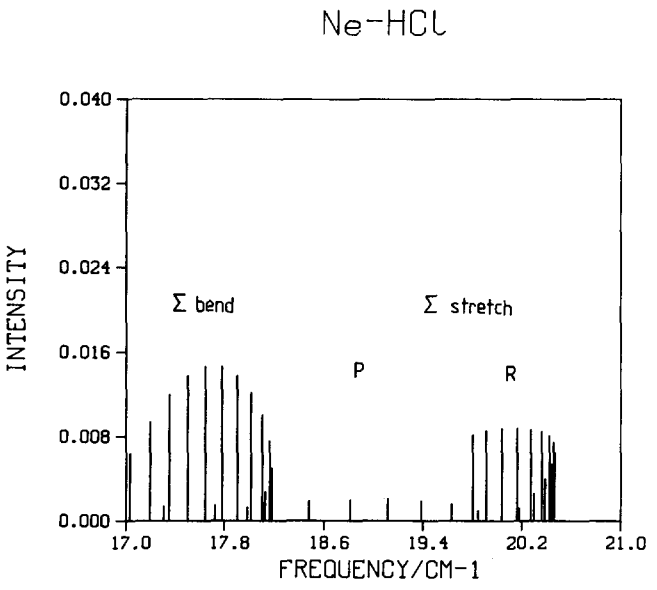

FIG. 3. Σ stretch of Ne–HCl (*P* and *R* branch) at 10 K. Also shown is the *R* branch of the Σ bend.

than that for the Σ bend. This small value of J reflects the fact that the rotor constant for the Σ stretching mode, 0.0750 cm^{-1} is even smaller than that for the Σ bending mode. The rotor constant for the Π bend, 0.091 25 cm^{-1}, is only slightly different from that for the fundamental and, furthermore, there is very little mixing induced by Coriolis coupling, between the Π bend and the Σ stretch. Consequently, as is shown in Fig. 4, the *P* and *R* branch show a regular structure. We do not display any lines for transitions involving $J > 10$ in the Π modes as these J states are dissociative, and will have quite large linewidths due to the more significant Coriolis coupling that exists for higher values of J. This is demonstrated in recent close-coupling calculations we have performed on the same modes in the analogous system Ne–HF.[40]

It is interesting to compare our calculated spectra with those measured[16] in the recent molecular beam experiments for a temperature close to 5 K. To do this we add the experimental frequency for the fundamental transition Ne–HCl($v = 0 \rightarrow 1$) to our calculated frequencies. Figure 5 shows a comparison of our calculated (5 K) and experimental spectrum for the *R* branch and part of the *P* branch for the Σ stretch. It can be seen that the experiment gives a bandhead in the *R* branch at $J = 4 \rightarrow 5$ while the calculation gives the bandhead at the $J = 5 \rightarrow 6$ transition. Furthermore, the relative intensities agree fairly well. A similar comparison for the *R* branch in the Σ bend is shown in Fig. 6, where the ^{22}Ne lines are also included. Here again the spectra compare well, with the ^{20}Ne–^{22}Ne shift being quite well reproduced in the calculations. Overall, the agreement between our calculated spectra and the experimental infrared spectra is surprisingly good, considering the fairly limited amount of information that produced the M4 potential. Clearly, this potential could be further refined with the new experimental data, although it should be remembered that the infrared spectra largely probe the Ne–HCl($v = 1$) part of the surface which will not be absolutely identical to that for Ne–HCl($v = 0$).

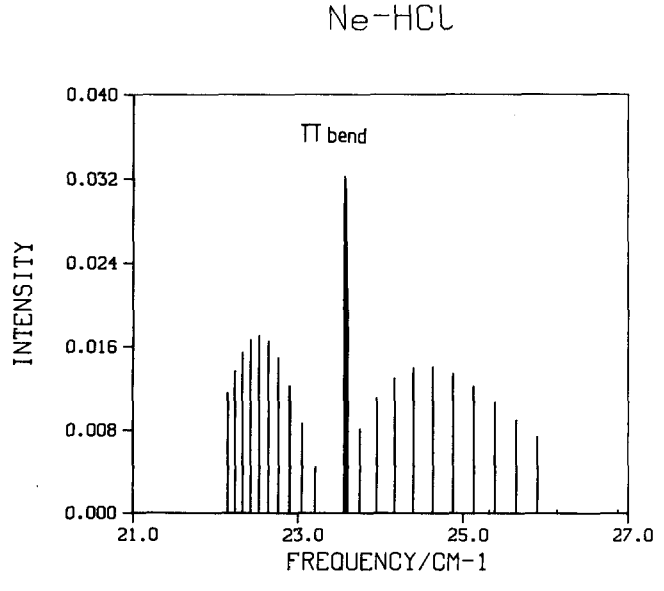

FIG. 4. Π bend of Ne–HCl (*P*, *Q*, and *R* branch) at 10 K.

B. Ar–HCl

Figure 7 shows the spectrum calculated for Ar–HCl at a temperature of 10 K. Comparison with the spectrum for Ne–HCl shows at once major differences. In particular, the fundamental band now has a much larger intensity while the relative intensity of the Σ bend is diminished. This reflects the more anisotropic potential for Ar–HCl giving a larger $j = 1$ basis function contribution to the fundamental level. Furthermore, on the scale of this spectrum, there is no obvious peak associated with the Σ stretch. This is because this mode now has a similar frequency to the Π bend and is hidden beneath the spectrum of that mode. Another interesting feature of the Ar–HCl spectrum is the relatively large intensities for bands with frequencies close to 70 cm^{-1}. These "overtone" levels correspond to states with an energy close to that for HCl($j = 2$) and are discussed in more detail below.

Figure 8 shows the enlarged portion of the spectrum corresponding to the Σ bend around 23.659 cm^{-1}. In this case there is no bandhead as the Σ stretch mode is not close in frequency to the Σ bend and the Σ bend is thus not strongly perturbed. In Fig. 9 an enlarged portion of the calculated spectrum around 34 cm^{-1} is shown. This shows the large intensities for the *P*, *Q*, and *R* branches of the Π bend. However, the *R* branch of the Σ stretch can also be observed beneath the *P* branch of the Π bend but with an intensity smaller by a factor of about 8. The Σ stretch borrows intensity in this case through Coriolis mixing which, by virtue of the near resonance with the Π^+ bend, is quite pronounced.

In Fig. 10 we show a comparison of the observed (infrared)[17] and calculated *P*, *Q*, and (partially) *R* branches in the region of the Σ stretch and Π bend absorption. Once again, the calculated frequencies have been changed by adding the fundamental experimental frequency for the Ar–HCl($v = 0 \rightarrow 1$) transition[17] to all the computed frequencies. The overall line positions and intensities of the observed and

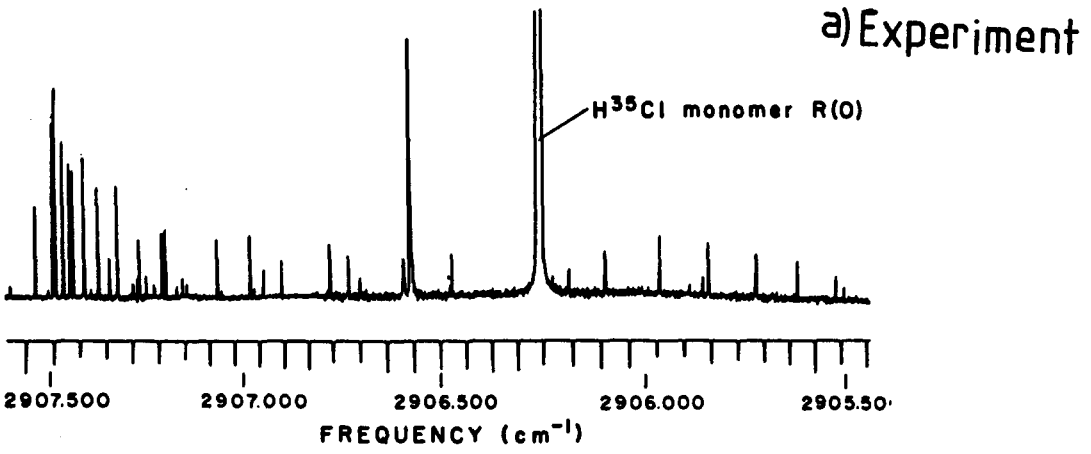

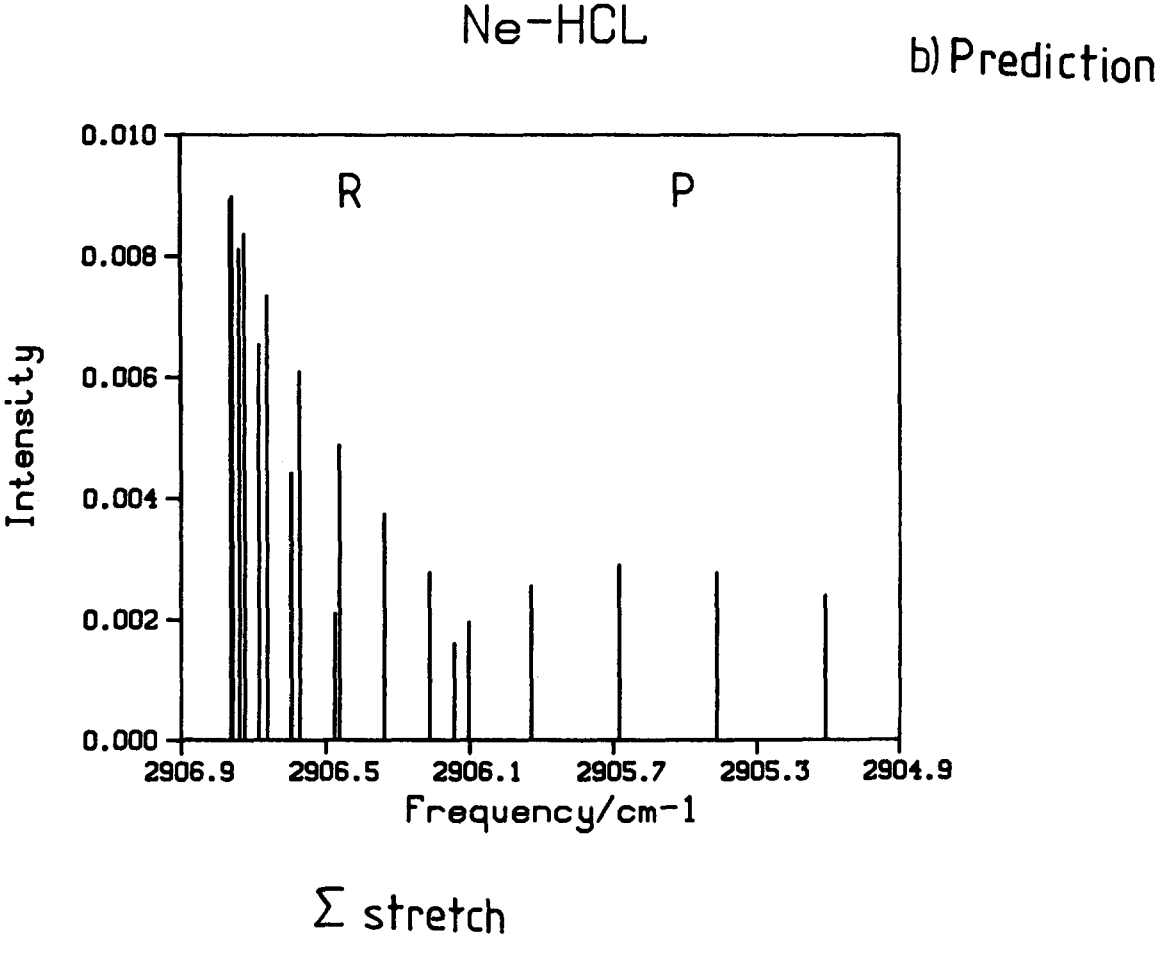

FIG. 5. Comparison of (a) experimental (Ref. 16) and (b) calculated spectrum for R and (partially) P branch of the Σ stretch of Ne–HCl at 5 K.

calculated spectra are gratifyingly close. However, some finer details differ. For example, the ratio between the experimental intensities for the corresponding $J \rightarrow J'$ transitions in the Σ stretch and Π bend is about 1:3, whereas the calculated ratio is about 1:8. It is possible that this difference is due to the fact that, in the Ar–HCl($v = 1$) state, the Σ stretch has a frequency slightly closer to the Π bend than that in Ar–HCl($v = 0$), and hence the mixing between these states will be slightly enhanced in Ar–HCl($v = 1$). Furthermore, the ratio of the calculated intensity for the Q branch of the Π bend to the P and R branch intensities is about the "normal" 2:1, whereas in the infrared experiment this ratio is closer to 1:1. It is also possible that these differences between theory and experiment are due to subtle features of the potential surface. After these calculations were completed, Hutson proposed another potential surface for Ar–

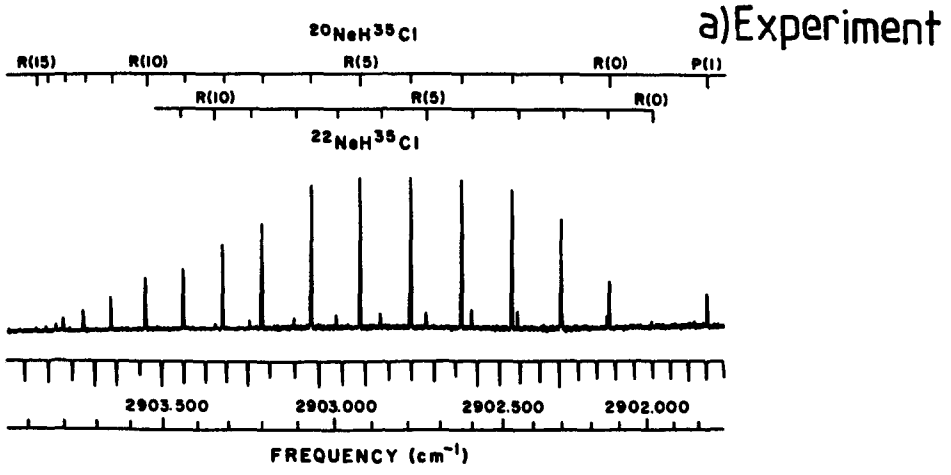

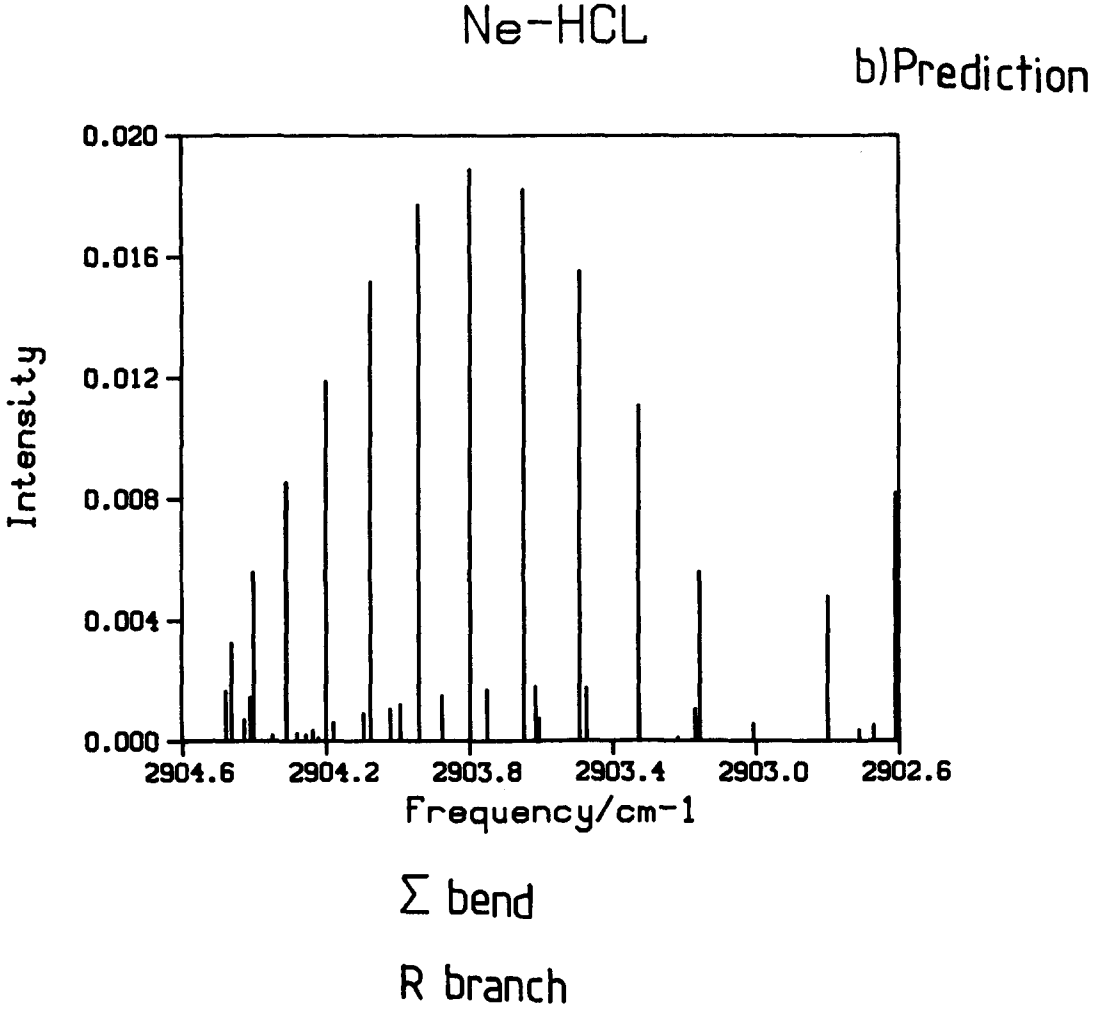

FIG. 6. Comparison of (a) experimental (Ref. 16) and (b) calculated spectrum for R branch of the Σ bend of Ne–HCl at 5 K.

HCl,[41] and we intend to repeat our calculations with this surface in the future. Also, our approximation of placing the dipole moment of the Ar–HCl along the HCl molecule will not be quite so accurate for Ar–HCl as it is for Ne–HCl, although large scale *ab initio* computations will be needed to investigate this aspect further. The infrared frequencies measured[17] for the Σ stretch, Σ bend, and Π bend transitions are 32.6374, 23.6289, and 34.0528 cm^{-1}, respectively, which de-

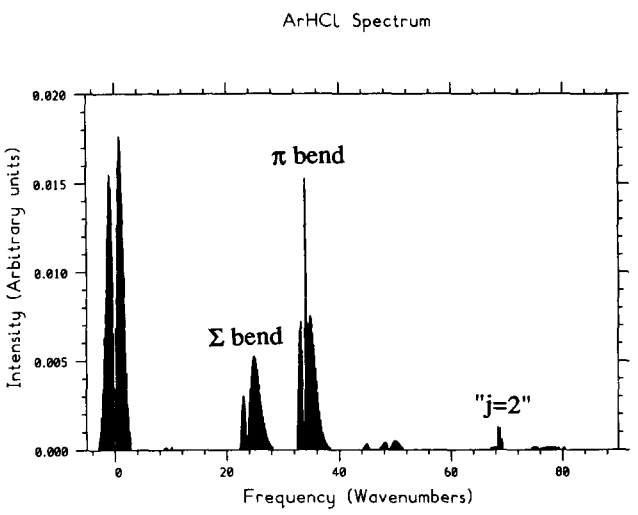

FIG. 7. Spectrum for Ar–HCl at 10 K. Notice the relatively large intensity of the bands close to 70 cm^{-1} corresponding to excitation of $j = 2$ bending overtones.

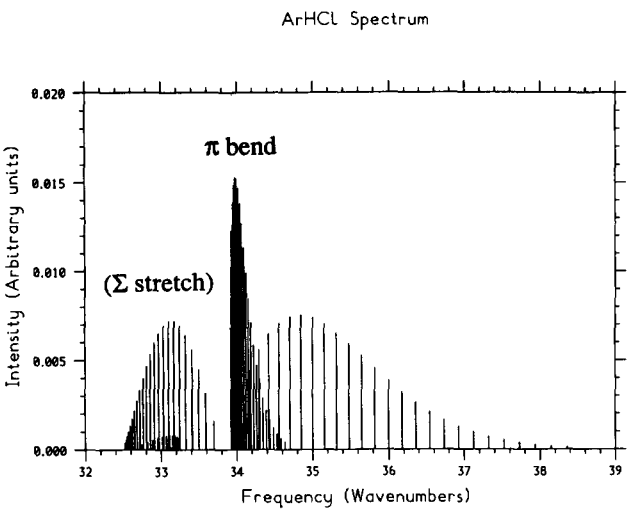

FIG. 9. Π bend of Ar–HCl (P, Q, and R branch) at 10 K. Beneath the P branch the lines with weaker intensity for the R branch of the Σ stretch can be seen.

viate by at most 0.2 cm^{-1} from those obtained with the M6C potential energy surface and those measured in the far-infrared experiment.[5–7]

An interesting, and somewhat novel feature, of the calculated spectrum for Ar–HCl shown in Fig. 7 are the relatively large intensities for the transitions centered near 70 cm^{-1}. These correspond to *overtone* transitions with a final state having quite a large doubly bend excited $j = 2$ component. Due to the strong anisotropy in the Ar–HCl potential, there is a reasonable amount of $j = 1$ character in these states also. There are three $j = 2$ basis functions with even parity and body-fixed projection quantum numbers 0–2, respectively. However, the Coriolis coupling between these states is so strong that the regular rotational spacings are lost and normal rotor constants cannot be assigned to these levels. This can be seen in Figs. 11 and 12. We emphasize also that due to the strong Coriolis mixing between these states quantum numbers, apart from J and p, cannot be sensibly assigned to them. Furthermore, at a frequency close to 75 cm^{-1} there are transitions associated with three quanta in the excited Σ stretching band and these borrow intensity from the Σ bend overtones. These overtone bands have not yet been seen experimentally but we predict that they certainly are intense enough to be observed. We note also that Tennyson[34] has performed previous energy level, although not intensity, calculations on Ar–HCl and he also finds extreme mixing between certain states which leads to "chaotic" spacings between energy levels.

Howard and Pine have also reported[10] infrared measurements of the Ar–HCl spectrum at a temperature of 127 K. A comparison between their spectra and those measured by Lovejoy and Nesbitt for 10 K has been made elsewhere,[17] and, therefore, we refrain from making such a comparison here. There are too many J states populated at 127 K for us to perform a proper simulation at that temperature. However, to examine the temperature dependence of the Ar–HCl spectrum in more detail we do report, in Fig. 13, the spectrum for 25 K. Comparison with the 10 K spectrum of Fig. 7 indicates the growth of hot bands largely associated with transitions out of the Σ bending mode. For example, the P, Q, and R branches close to 10 cm^{-1} are associated with the transition Σ bend → Π bend, which has a particularly strong intensity and could even just be observable at 10 K. Furthermore, the bands around 45 cm^{-1} are associated with the transition from the Σ bend to the $j = 2$ levels discussed above and these should certainly be observable at higher temperatures. Comparisons of Figs. 7 and 13 are a good example of how an increase in temperature can lead to quite considerable congestion in certain regions of the spectrum.

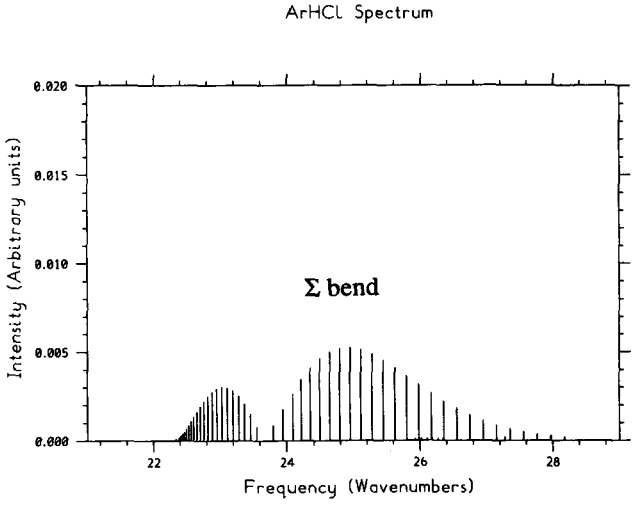

FIG. 8. Σ bend of Ar–HCl (P and R branch) at 10 K.

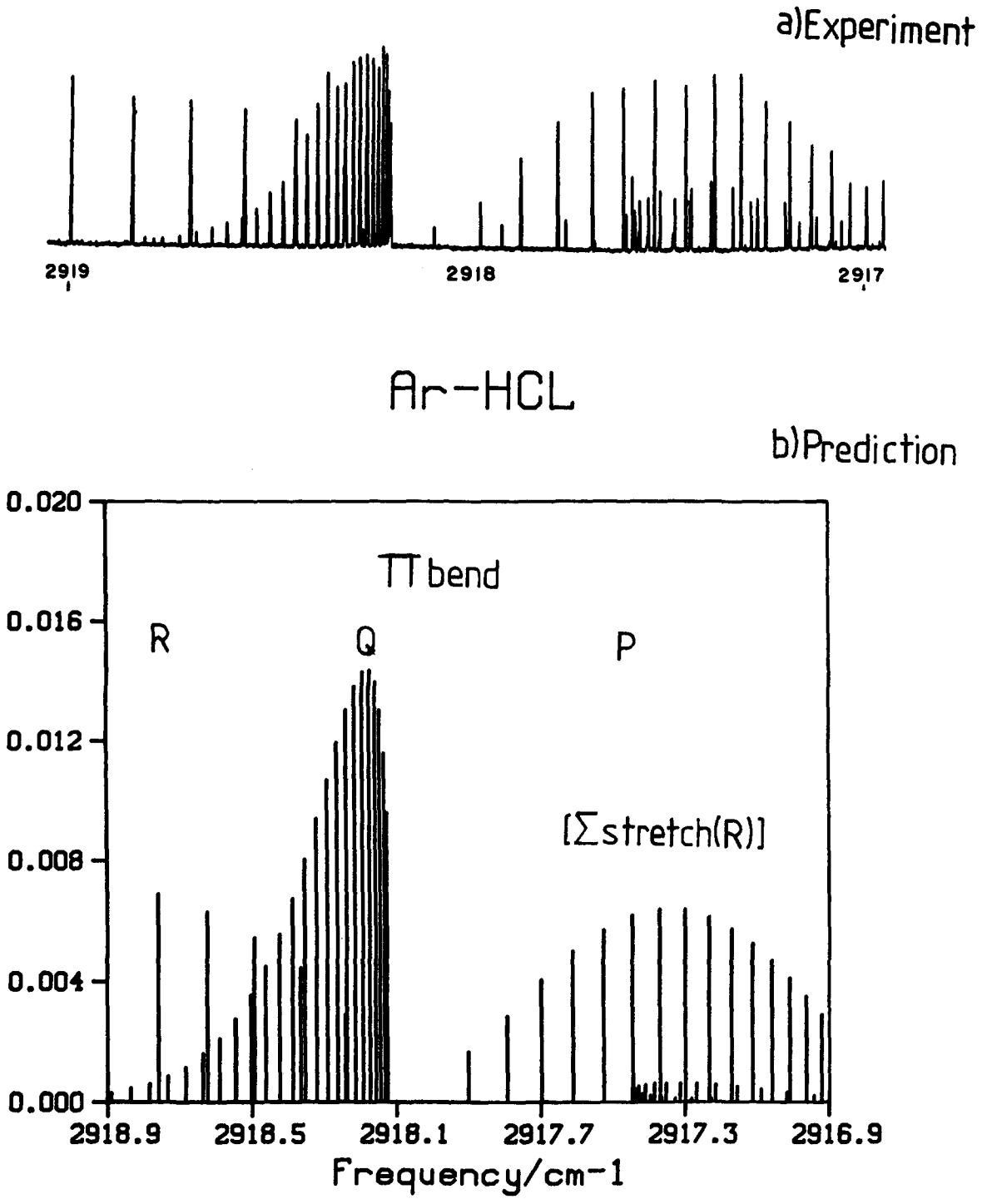

FIG. 10. Comparison of (a) experimental (Ref. 17) and (b) calculated spectrum for R, Q, and P branch of the Π bend of Ar–HCl at 10 K. Also seen, with lower intensity beneath the P branch of the Π bend, is the R branch of the Σ stretch.

C. Kr–HCl and Xe–HCl

No far-infrared or infrared high-resolution measurements have yet been made for the Kr–HCl and Xe–HCl complexes. This is partly due to the fact that the large number of available isotopes for Kr and Xe ensure many overlapping lines. Figures 14 and 15 show the spectra for Kr–HCl and Xe–HCl, respectively. These follow the trends noticed for Ne–HCl and Ar–HCl. The fundamental mode has an intensity that increases with the mass of the rare gas atom, while the Σ bend intensity decreases. This is associated with an increase in anisotropy in the potential energy surface along the series. The Σ bend correlates with the level (02^00) in normal mode triatomic notation and, in the limit of extreme anisotropy and large well depth, the transition intensity to this level from (00^00) will be almost zero. Furthermore, the overtone transition intensities into the "$j = 2$" states become larger as the mass of the rare gas atom increases.

Figures 16 and 17 show enlarged spectra for these overtone transitions for Kr and Xe, respectively. Examination of

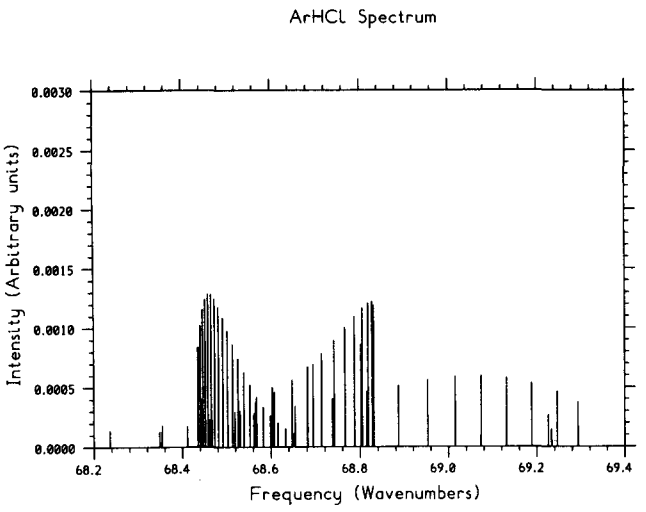

FIG. 11. Bending overtone ($j = 2$) band of Ar–HCl close to 69 cm^{-1}. Here the levels are strongly mixed by Coriolis coupling.

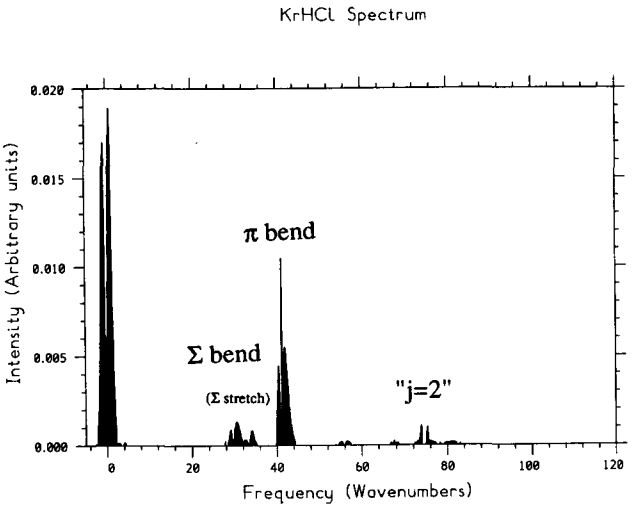

FIG. 14. Spectrum for Kr–HCl at 10 K.

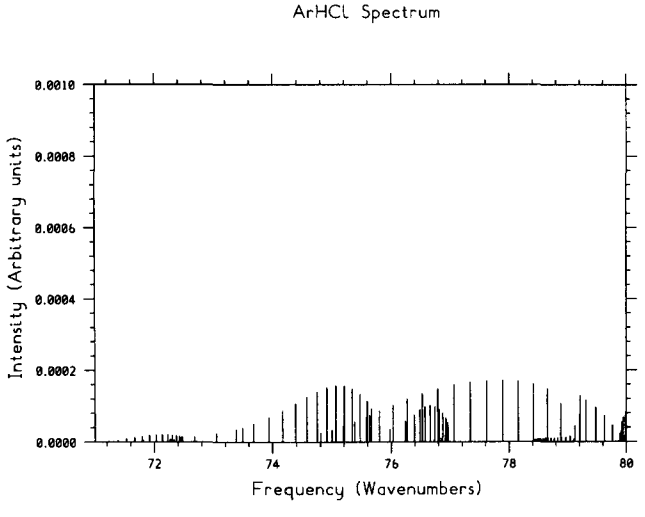

FIG. 12. Bending overtone ($j = 2$) band of Ar–HCl close to 76 cm^{-1}.

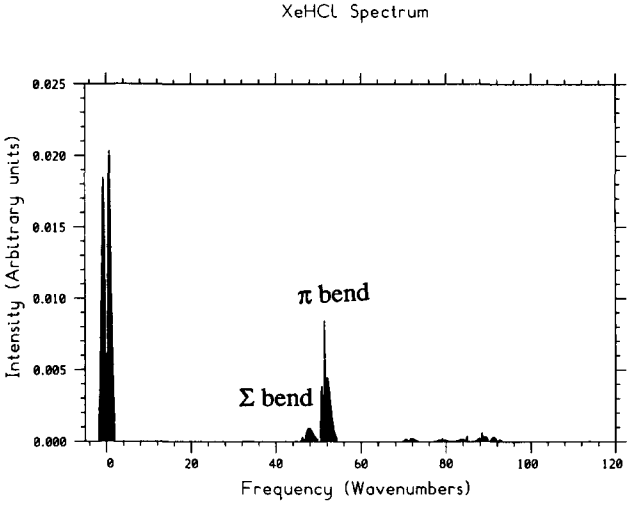

FIG. 15. Spectrum for Xe–HCl at 10 K.

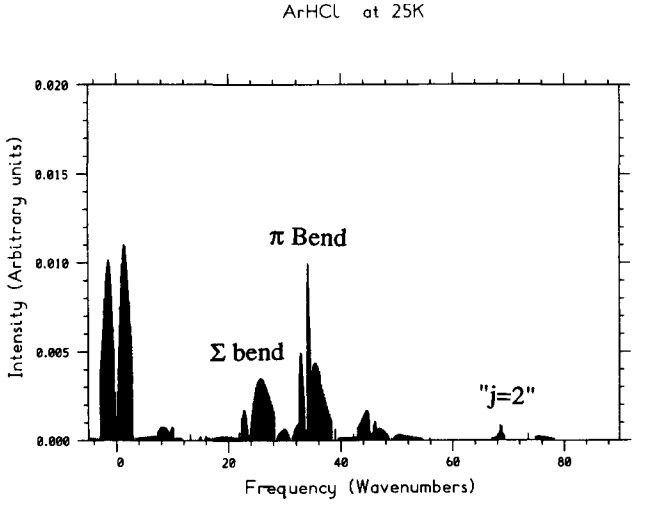

FIG. 13. Spectrum for Ar–HCl at 25 K. Comparison with Fig. 7 illustrates the appearance of hot bands.

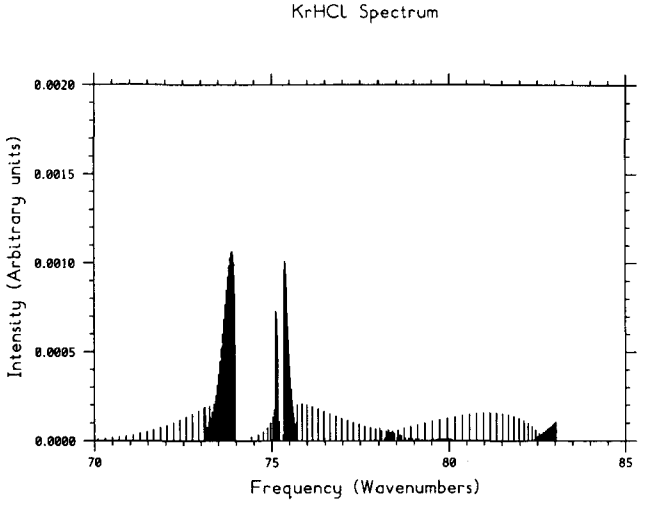

FIG. 16. Bending overtone ($j = 2$) bands for Kr–HCl.

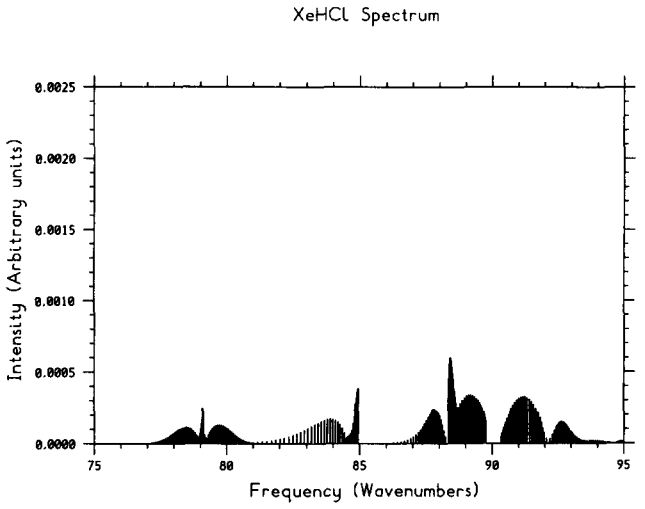

FIG. 17. Bending overtone ($j = 2$) bands for Xe–HCl.

the Kr spectrum in Fig. 16 shows that the band close to 73 cm^{-1} has only a P and R branch while those close to 75 and 88 cm^{-1} also have Q branches. Thus, the body-fixed quantum numbers $K = 0$, 1, and 2 can be reasonably associated with the final states in these transitions.

It is interesting not only to look at the calculated spectra but also at the calculated wave functions. This can put on more quantitative terms the ideas about mixing of j-labeled basis functions referred to above. To examine this feature, we show in Fig. 18 the leading basis function coefficients in the angular wave function with lowest energy level for $J = 5$. Thus, the angular wave function of Eq. (8) is expanded in the form

$$\Psi^{0-}_{\text{ang}} = d_{50}\, y^{50-}_{50} + d_{41} y^{50-}_{41} + d_{72}\, y^{50-}_{72} + \cdots , \qquad (14)$$

where the basis function y^{JMp}_{lj} is defined in Eq. (7). Since this is the ground state wave function, the size of the coefficients d_{lj} will reflect the mixing in of the different j states, which will, itself, be reflected in the transition intensities into and out of the fundamental band. It can be seen in Fig. 18 that the $j = 1$ and $j = 2$ coefficients increase quite considerably along the series Ne, Ar, Kr, Xe and thus the increase in the intensity for both the fundamental and $j = 2$ overtone bands along this series, which is observed in the calculation, is to be expected.

To examine this point in more detail, a correlation diagram is presented in Fig. 19. This shows how the bending energy levels for $J = 2$ of a model Ar–HCl complex vary with the anisotropy terms in the potential V_1 and V_2, where the angular potential is expanded as

$$V = V_1 P_1(\cos\theta) + V_2 P_2(\cos\theta) . \qquad (15)$$

For zero anisotropy in the potential, $j = 0$, 1, and 2 are good quantum numbers, while, with very large magnitudes for V_1 and V_2, the simple harmonic quantum number notation $(n_1 n_2^{l} n_3)$ is appropriate. This is illustrated on the diagram. For the Ar, Kr, and Xe complexes, V_1 and V_2 are in the range -50 to -150 cm^{-1} which is the region where there are strong avoided crossings in the rotationally adiabatic potential curves, and strong mixings between the different j states. Thus, neither the j notation or the $(n_1 n_2^{l} n_3)$ notation are really appropriate for these complexes. For the Ne–HCl complex the V_1 and V_2 coefficients are smaller and the j notation is more appropriate—the $j = 2$ bands do not have strong intensities in this case. Note that in the limit of a very strong anisotropy and deep well in the potential, the $j = 2$ bands will diminish in intensity as will the Σ bend transition since these states correlate with bending overtones in the nearly rigid molecule limit. In this case only the transition from the ground state into $(01^{1}0)$ will be allowed.

VI. CONCLUSIONS

We have described calculations of the J-dependent spectra for the excitation of the low-lying bending and stretching modes in complexes of the rare gases Ne, Ar, Kr, and Xe with HCl. We have attempted to use the best potentials available to us at the time the project was initiated. The results are relevant to high resolution far-infrared and infrared measurements, and particularly those made at low temperatures using molecular beams.

The main new feature of this work is the prediction of the full J-dependent intensities for all the possible transitions

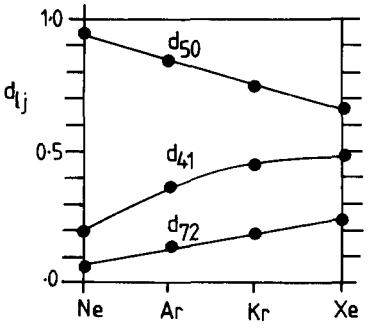

FIG. 18. Plot of basis function coefficients d_{lj}, with $j = 0$, 1, and 2 for Ne, Ar, Kr, and Xe [see Eq. (14)].

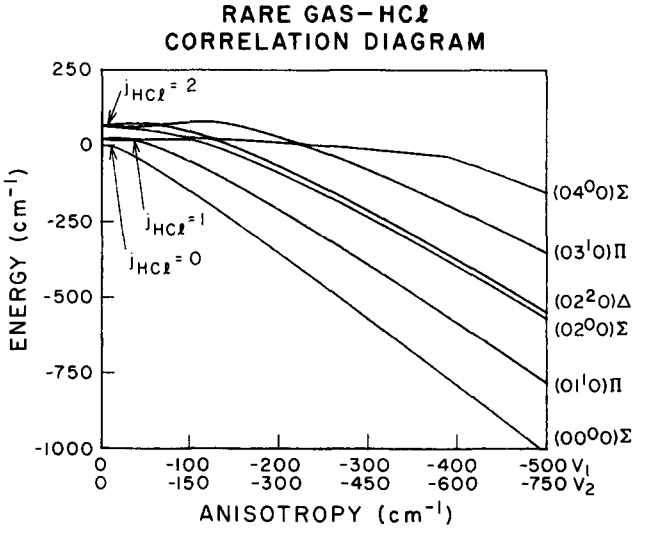

FIG. 19. Correlation diagram for the bending energy levels of a rare gas–HCl complex. The energies are plotted as a function of the anisotropy terms in the potential V_1 and V_2 of Eq. (15). With zero anisotropy, the j labeling of the levels is applicable, while, with very strong anisotropy, the linear triatomic simple harmonic oscillator notation $(n_1 n_2^{l} n_3)$ is appropriate.

at temperatures close to 10 K. Indeed, we find that our calculated intensities and spectra agree markedly well with the infrared spectra measured for Ne–HCl, and Ar–HCl. An interesting feature arising out of this work is the prediction of quite large intensities for overtone transitions in the Ar, Xe and Kr–HCl complexes associated with levels correlating with HCl($j = 2$) states. It seems very likely that infrared measurements of these transitions should be feasible and our results suggest strongly that they should reveal interesting spectral congestions associated with large Coriolis couplings.

The basis function technique that we have used is very straightforward and automatic to apply and our computer program should be applicable to many other atom–diatom complexes. For example, we have found it easy to use the same program in calculations on Ne–HF[40] and Ar–HF.[43] Furthermore, the extension to diatom–diatom and atom–triatom complexes will be quite possible. For calculations on the fundamental bands for a limited number of low J values, the close-coupling approach will still be the method that will give the highest accuracy. However, when calculations of transition intensities and spectra are required, the basis set approach would appear to have significant advantages and, with appropriate dynamical approximations, will be extendable to systems larger than triatomics. We are currently extending the approach described here to diatom–diatom complexes such as H_2–HF which have also been the study of detailed infrared measurements.[15]

ACKNOWLEDGMENTS

We would like to thank Dr. J. M. Hutson for permission to use his unpublished M6C potential for Ar–HCl. We would also like to thank Dr. D. D. Nelson, Jr. for computational assistance. This work was supported by the National Science Foundation under Grant Nos. PHY86-04504 and CHE86-05970.

[1]T. R. Dyke, in *Hydrogen Bonds*, edited by P. Schuster (Springer, New York, 1984), p. 85.
[2]*Structure and Dynamics of Weakly Bound Molecular Complexes*, edited by A. Weber (Reidel, Dordrecht, 1987).
[3]M. D. Marshall, A. Charo, H. O. Leung, and W. Klemperer, J. Chem. Phys. **83**, 4924 (1985).
[4]D. Ray, R. L. Robinson, D.-H. Gwo, and R. J. Saykally, J. Chem. Phys. **84**, 1171 (1986).
[5]R. L. Robinson, D.-H. Gwo, D. Ray, and R. J. Saykally, J. Chem. Phys. **86**, 5211 (1987).
[6]R. L. Robinson, D. Ray, D.-H. Gwo, and R. J. Saykally, J. Chem. Phys. **87**, 5149 (1987).
[7]R. L. Robinson, D.-H. Gwo, and R. J. Saykally, J. Chem. Phys. **87**, 5156 (1987).
[8]K. L. Busarow, G. A. Blake, K. B. Laughlin, R. C. Cohen, Y. T. Lee, and R. J. Saykally, Chem. Phys. Lett. **141**, 289 (1987).
[9]A. S. Pine, W. J. Lafferty, and B. J. Howard, J. Chem. Phys. **81**, 2939 (1984).
[10]B. J. Howard and A. S. Pine, Chem. Phys. Lett. **122**, 1 (1985).
[11]A. S. Pine and B. J. Howard, J. Chem. Phys. **84**, 590 (1986).
[12]G. T. Fraser and A. S. Pine, J. Chem. Phys. **85**, 2502 (1986).
[13]C. M. Lovejoy, M. D. Schuder, and D. J. Nesbitt, J. Chem. Phys. **85**, 4890 (1986).
[14]C. M. Lovejoy and D. J. Nesbitt, J. Chem. Phys. **86**, 3151 (1987).
[15]C. M. Lovejoy, D. D. Nelson, Jr., and D. J. Nesbitt, J. Chem. Phys. **87**, 5621 (1987).
[16]C. M. Lovejoy and D. J. Nesbitt, Chem. Phys. Lett. **147**, 490 (1988).
[17]C. M. Lovejoy and D. J. Nesbitt, Chem. Phys. Lett. **146**, 582 (1988).
[18]S. L. Holmgren, M. Waldman, and W. Klemperer, J. Chem. Phys. **69**, 1661 (1978).
[19]A. M. Dunker and R. G. Gordon, J. Chem. Phys. **64**, 354 (1976); **68**, 700 (1978).
[20]J. M. Hutson and B. J. Howard, Mol. Phys. **43**, 493 (1981).
[21]J. M. Hutson and B. J. Howard, Mol. Phys. **45**, 769 (1982).
[22]C. J. Ashton, M. S. Child, and J. M. Hutson, J. Chem. Phys. **78**, 4025 (1983).
[23]J. M. Hutson, J. Chem. Phys. **81**, 2357 (1984).
[24]J. M. Hutson, J. Chem. Soc. Faraday Trans. 2 **82**, 1163 (1986).
[25]G. Danby, J. Phys. B **16**, 3393 (1983).
[26]D. E. Manolopoulos, J. Chem. Phys. **85**, 6425 (1986); D. E. Manolopoulos, Ph.D. thesis, University of Cambridge, 1988.
[27]S. Carter and N. C. Handy, Comput. Phys. Rep. **5**, 115 (1986).
[28]G. Brocks, J. Chem. Phys. **88**, 578 (1988).
[29]J. Tennyson and A. van der Avoird, J. Chem. Phys. **77**, 5664 (1984); G. Brocks and A. van der Avoird, Mol. Phys. **55**, 11 (1985).
[30]B. P. Reid, K. C. Janda, and N. Halberstadt, J. Phys. Chem. **92**, 587 (1988).
[31]J. M. Hutson (private communication, 1987).
[32]A. M. Arthurs and A. Dalgarno, Proc. R. Soc. London Ser. A **256**, 540 (1960).
[33]J. T. Yardley, *Introduction to Molecular Energy Transfer* (Academic, New York, 1980).
[34]J. Tennyson, Mol. Phys. **55**, 463 (1985).
[35]I. P. Hamilton and J. C. Light, J. Chem. Phys. **84**, 306 (1986).
[36]D. M. Brink and G. R. Satchler, *Angular Momentum* (Clarendon, Oxford, 1962).
[37]P. W. Fowler and A. D. Buckingham, Mol. Phys. **50**, 1349 (1983).
[38]R. D. Amos, Mol. Phys. **35**, 1765 (1978).
[39]G. C. Maitland and E. B. Smith, Chem. Phys. Lett. **22**, 443 (1973).
[40]D. C. Clary, C. M. Lovejoy, S. V. O Neil, and D. J. Nesbitt, Phys. Rev. Lett. **61**, 1576 (1988).
[41]J. M. Hutson, J. Chem. Phys. **89**, 4550 (1988).
[42]J. Tennyson, Comput. Phys. Rep. **4**, 1 (1986).
[43]M. S. Child, D. J. Nesbitt, and D. C. Clary, J. Chem. Phys (in press).